D-6-06

Extended Abstracts of the 2019 International Conference on Solid State Devices and Materials, Nagoya, 2019, pp207-208

Controlling Color Conversion Efficiency between Monolayer Tungsten Diselenide and Quantum Dots through Plasmonic Effect of Silver Nanodisks Metasurface

Andrew Boyi Lee[1], Chen-An Lin[2], Chiao-Yun Chang[1], Cheng-Li Yu[1], Hsiang-Ting Lin[1], Hao-Chung Kuo[2], Min-Hsiung Shih[1,2]

[1] Research Center for Applied Sciences (RCAS), Academia Sinica
128 Academia Road, Section 2, Nangang, Taipei 11529, Taiwan, ROC.
[2] National Chiao Tung Univ. 1001 University Road, Hsinchu 30010, Taiwan, ROC.
Phone: +886-2-2787-3184
E-mail: mhshih@gate.sinica.edu.tw

Abstract

The atomic scale transition metal dichalcogenides (TMDCs) material could be a potential role of miniature light emitting devices (LED).The fabrication of Ag nanodisks (NDs) arrays of plasmonic metasurface structure and the resonance wavelength of Ag nanodisks (NDs) metasurface could actually be manipulated by varying the diameter size of Ag NDs. The plasmon enhancement factor of monolayer tungsten diselenide (WSe_2) and CdSe/quantum dots (QDs) with different resonance wavelengths of Ag NDs metasurfaces are investigated. Besides, we successfully demonstrated controlling light conversion efficiency between QDs and WSe_2 through plasmonic metasurfaces and suggested that the TMDCs has the potential to be applied to light emitting devices or display technology such as white light emitting diodes (WLEDs) with the support of localized surface plasmon resonance (LSPR).

1. Introduction

The transition metal dichalcogenides (TMDCs) materials own higher quantum yield compared with other two dimensional materials, which could be a potential role of miniature light emitting devices (LED). However, TMDCs still have their limitation to practically apply for the light-emitting devices since the quantum yields of TMDCs are relatively lower than traditional semiconductors. The surface plasmon effect has a strong electric field at the interface that is expected to interact with the optical properties of TMDCs materials in the neighbourhood of the metal nanostructures[1]. The effect could promote the absorption and emission at specific resonance frequency, and hence directly enhance color conversion and light emission efficiency. Besides, the CdSe/QDs benefit from its size-tunability, broadband absorption, narrow emission spectra, high quantum yield, high color purity, and easy manufacturing[2]. In the first and second part, we focus on the fabrication of Ag nanodisks (NDs) metasurfaces structure and design the Ag ND metasurfaces with desired resonant wavelengths by finite element method. In the third part, we utilized the Ag ND metasurfaces combined with CdSe/QDs and monolayer tungsten diselenide (WSe_2) to enhance the emission of monolayer WSe_2 as well as convert the light from QDs to WSe_2. In the future, utilizing plasmonic metasurface integrated with the TMDCs and CdSe/QDs emitting visible light with the GaN-based LED could helpfully achieve white light emitting device.

2. Experiments and Results

2.1 Fabrication

First, the monolayer WSe_2 grown on sapphire by chemical vapor deposition (CVD) was transferred onto silica substrate by wet transfer. In addition, Al_2O_3 thin film with thickness of 5 nm was deposited by atomic layer deposition (ALD) system as the dielectric layer to prevent direct contact with arrays. To achieve a series of fabricating Ag ND metasurfaces with different resonance wavelengths, PMMA A3 and PMMA A5 were spin-coated on top of the sample as the photoresist, and then the patterns of Ag ND arrays were defined by e-beam lithography and later the sample was developed by MIBK solution. Afterwards, e-gun evaporation was utilized to deposit 5 nm of titanium for adhesion layer and 70 nm of Ag on the sample. Further, the Ag ND metasurfaces were obtained by lift-off process of bilayer photoresist and again 5 nm of Al_2O_3 thin film was deposited by ALD system. Finally, the CdSe/QDs were spray-coated on the metasurfaces, as schematically shown in Fig. 1(a). Fig. 1(b) illustrates the top view scanning electron microscope (SEM) image of Ag ND metasurfaces. The size of diameter and period, noted D and P in Fig. 1(b), respectively, of Ag ND metasufaces can be controlled by the fabrication through e-beam lithography patterning. Fig. 1(c) shows the cross-section transmission electron microscope (TEM) image of the sample. Atomic thickness of monolayer WSe_2 exhibits on the silica substrate and also QDs could be seen on the Ag ND metasurfaces.

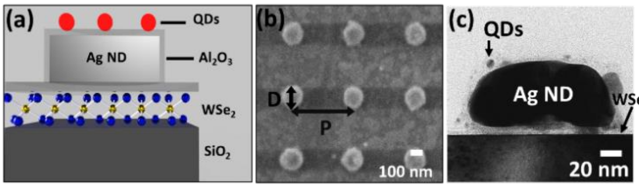

Fig. 1(a) The schematic diagram of cross section with WSe_2 and CdSe/QDs consisting of Ag ND metasurfaces. (b) The top view SEM image of Ag ND metasurfaces. (c) The cross-section TEM image of Ag ND with WSe_2 and Cd/Se QDs. Inset: magnification of monolayer WSe_2.

2.2 Tuning Resonance Wavelength of Ag Nanodisk Metasurfaces

The resonance wavelength of the Ag ND metasurfaces could be estimated the resonant wavelength by finite element method (FEM). By tuning diameter of the Ag ND metasurfaces, transmission spectrum and resonant wavelength versus diameter could be acquired. In addition, Fig. 2(a) presents the measured results of transmission spectrum, and the peak value of each transmission line could be clarified the relation between resonant wavelength and diameter of nanodisks, as shown in Fig 2(b). The diameter size of nanodisks that could be tuned from 110 nm to 250 nm indicates the resonant wavelength could be manipulated from 520 nm to 760 nm. Hence, with the support of simulation and measured results, the resonant wavelength could be successfully dominated and also expand to involve target materials, WSe_2 and CdSe/QDs.

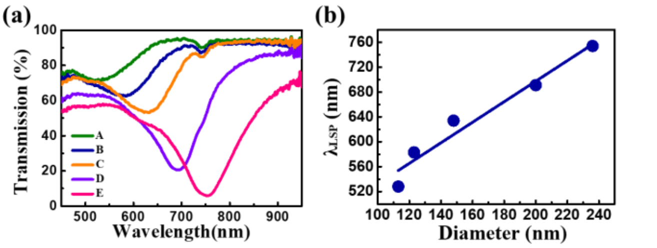

Fig. 2 The measured results of Ag ND metasurfaces of (a) transmission spectrum and (b) resonant wavelength versus diameter.

2.3 Color Conversion between WSe_2 and Quantum Dots (QDs)

In Fig. 3(a), the right side of y-axis displays normalized absorption spectrum of Ag ND with resonance wavelength being 630 nm on silica substrate and the broadband absorption covers the emission wavelength of 630 nm CdSe/QDs and 750 nm WSe_2. Moreover, the left side y-axis of Fig. 3(a) illustrates the photoluminescence (PL) spectrum of WSe_2 with the Ag ND metasurfaces. It also includes the PL spectrum of CdSe/QDs, WSe_2, and both WSe_2 + CdSe/QD with the Ag NDs. It is clear to discover that the emission intensity of WSe_2 increases after adding CdSe/QDs, as indicated by the orange arrow in Fig. 3(a), which was probably caused by the light transfer from CdSe/QDs to WSe_2 by Ag metasurfaces because the intensity of CdSe/QDs integrated with metasurfaces descends significantly after combining WSe_2, as also indicated by the brown arrow in Fig. 3(a). In addition, owing to the surface plasmon effect of metasurfaces, the intensity of WSe_2 enhances slightly. The plasmon enhancement factor of WSe_2 (EF_{WSE2}) , as shown in eq. (1), is calculated by the ratio of integrated area emission intensity of the WSe_2 monolayer with and without Ag NDs.

$$EF_{WSe2} = \frac{\int_{700}^{850} Int_{Ag\ ND+WSe2} d\lambda}{\int_{700}^{850} Int_{WSe2} d\lambda} \tag{1}$$

Similarly, the plasmon enhancement factor of CdSe/QDs is also calculated written in the same equation with different notation EF_{QDs} and Int_{QDs}. The highest plasmon enhancement of WSe_2 and CdSe/QDs are 3.1 and 12.4 times in the samples, respectively. Besides, the color conversion efficiency equation is shown in eq. (2) as the following:

$$\eta = \frac{\int_{700}^{850} Int_{QDs+AgND+WSe2} d\lambda - \int_{700}^{850} Int_{AgND+WSe2} d\lambda}{\int_{580}^{700} Int_{QDs+AgND} d\lambda - \int_{580}^{700} Int_{QDs+AgND+WSe2} d\lambda} \tag{2}$$

The symbols of $Int_{QDs+AgND+WSe2}$, $Int_{Ag\ ND+WSe2}$, and $Int_{QDs+Ag\ ND}$ represent the intensity of pink, green, and blue solid line in Fig. 3(a), respectively. After calculating the color conversion efficiency of the samples, the schematic η–λ_{LSP} diagram, as shown in Fig. 3(b) could determine the best choice of the Ag ND for color conversion. It indicates that the sample with resonant wavelength being 653 nm has the highest conversion efficiency of 52.7%, and the sample with resonant wavelength being 760 nm does not show any conversion. The explanation of the results is that the color conversion process involves emission of CdSe/QDs, the absorption of CdSe/QDs emitted by WSe_2, and emission of WSe_2. Therefore, due to its absorption spectrum, the sample with resonant wavelength being 653 nm has the most ideal overlap with CdSe/QDs and WSe_2 simultaneously, which facilitates all the effects in color conversion.

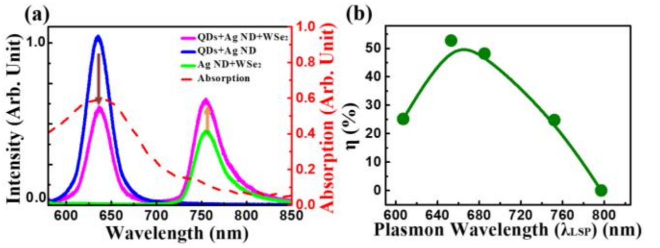

Fig. 3(a) The absorption spectra of Ag NDs metasurface (red dash line) and the PL spectrum of WSe_2 (green line), CdSe/QDs (blue line) combined with metasurface, both WSe_2 and CdSe/QDs integrated with metasurface (pink line). (b) The color conversion efficiency versus plasmon resonant wavelength.

3. Conclusions

We successfully fabricated Ag ND metasurfaces with fine tuning resonant wavelength and also studied the enhacement factor of monolayer WSe_2 and CdSe/QDs. The plasmon effect enhanced the color conversion efficiency between CdSe/QDs and monolayer WSe_2 with Ag NDs metasurfaces. The PL enhancement of WSe_2 accompanying with decresing PL intensity of CdSe/QDs presented the color conversion due to its absorption spectrum of Ag ND had the most ideal overlap with CdSe/QDs and WSe_2 simultaneously, which facilitated all the effects in color conversion. The high efficiency from the light emission of CdSe/QDs to WSe_2 as intermediate was estimated approximately 52.7% with the resonant wavelength being 653 nm. In the future, utilizing plasmonic metasurface integrated with the TMDCs and CdSe/QDs emitting visible light with the GaN-based LED could helpfully achieve white light emitting device.

Acknowledgements

This work has been supported by the Ministry of Science and Technology (MOST) in Taiwan under Contract Nos. No. 105-2112-M-001-011-MY3.

References

[1]S. Butun, E. Palacios, J.D. Cain, Z. Liu, V.P. Dravid and K. Aydin, ACS Appl Mater Interfaces. **9** (2017) 15044.

[2]M.X. Zhao and E.Z. Zeng, Nanoscale Res Lett. **10** (2015) 171.

[3]C.Y. Liu, T.P. Chen, T.S. Kao, J.K. Huang, H.C. Kuo, Y.F. Chen and C.Y. Chang, Opt Express. **24** (2016) 19978.